Cu(II)-Incorporated, Histidine-Containing, Magnetic-Metal-Complexing Beads as Specific Sorbents for the Metal Chelate Affinity of Albumin

Sinan Akgöl, Deniz Türkmen, Adil Denizli

Biochemistry Division, Department of Chemistry, Hacettepe University, Beytepe, Ankara, Turkey

Received 27 July 2003; accepted 18 February 2004
DOI 10.1002/app.20757
Published online in Wiley InterScience (www.interscience.wiley.com).

ABSTRACT: *N*-Methacryloyl-(L)-histidine methyl ester (MAH) was synthesized from metharyloyl chloride and histidine. Spherical beads with an average size of 150–250 μm were obtained by the suspension polymerization of ethylene glycol dimethacrylate and MAH in an aqueous dispersion medium. Magnetic poly(ethylene glycol dimethacrylate-*co*-*N*-Methacryloyl-(L)-histidine methyl ester) [m-p(EGDMA-*co*-MAH)] microbeads were characterized with swelling tests, electron spin resonance, elemental analysis, and scanning electron microscopy. The specific surface area of the beads was 80.1 m^2/g. m-p(EGDMA-*co*-MAH) microbeads with a swelling ratio of 40.2% and 43.9 μmol of MAH/g were used for the adsorption of bovine serum albumin (BSA) in a batch system. The Cu(II) concentration was 4.1 μmol/g. The adsorption capacity of BSA on the Cu(II)-incorporated beads was 19.2 mg of BSA/g. The BSA adsorption first increased with the BSA concentration and then reached a plateau, which was about 19.2 mg of BSA/g. The maximum adsorption was observed at pH 5.0, which was the isoelectric point of BSA. The BSA adsorption increased with decreasing temperature, and the maximum adsorption was achieved at 4°C. High desorption ratios (>90% of the adsorbed BSA) were achieved with 1.0*M* NaSCN (pH 8.0) in 30 min. The nonspecific adsorption of BSA onto the m-p(EGDMA-*co*-MAH) beads was negligible. © 2004 Wiley Periodicals, Inc. J Appl Polym Sci 93: 2669–2677, 2004

Key words: magnetic polymers; seperation techniques; proteins; tyrosine

INTRODUCTION

Human serum albumin is the most abundant protein in blood plasma. It has many important physiological functions that contribute significantly to the colloid osmotic blood pressure and aid in the transport, distribution, and metabolism of many endogenous and exogenous substances, including bile acids, bilirubin, long-chain fatty acids, amino acids (notably tryptophan, tyrosine, and cysteine), steroids (progesterone, testosterone, aldosterone, and cortisol), metal ions such as copper, zinc, calcium, and magnesium, and numerous pharmaceuticals.[1] Human serum albumin consists of a single, nonglycosylated polypeptide chain containing 585 amino acid residues. Its amino acid sequence contains a total of 17 disulfide bridges, one free thiol, and a single tryptophan.[2] Research on albumin separation has attracted considerable attention for its great potential in manufacturing blood protein. Human serum albumin is at present commonly isolated from human plasma by Cohn's classical blood fractionation procedure.[3] Cohn's method involves the precipitation of proteins with ethanol with various pHs, ionic strengths, and temperatures. However, this technique, which is the oldest industrial method of fractionating blood proteins, is not highly specific and can yield partially denatured proteins.[4] The rapid development of biotechnology, biochemistry, pharmaceutical science, and medicine requires more reliable and efficient separation techniques for the isolation and purification of biomolecules such as proteins, enzymes, peptides, nucleic acids, and hormones.[5–6]

Bioaffinity chromatography is already a well-established method for the identification, purification, and separation of biomolecules and is based on highly specific molecular recognition or biorecognition. In this method, a molecule possessing a specific recognition capability (i.e., ligand) is immobilized on a suitable insoluble support, which is usually a polymeric material in bead or membrane form.[7] The molecule to be isolated is selectively captured by the complementary ligand immobilized on the matrix. Bioaffinity chromatography is an alternative technique to Cohn's fractionation. Biological ligand stability is becoming an increasingly important consideration. The trend, therefore, has been to replace high-molecular-mass biological ligands with low-molecular-mass pseudo-specific ligands.[8,9]

In particular, small amino acid ligands offer advantages over biological ligands in terms of economy,

Correspondence to: S. Akgöl.

ease of immobilization, chemical stability, and high adsorption capacity.[6–11] The idea of using different amino acids stems from the fact that amino acids are very reactive to different chemical substances, including metal ions and proteins. The higher flexibility and durability of these amino acid ligands, as well as the significantly lower material and manufacturing costs, are also very important. In addition, amino acids may be easily modified with existing chemical methods to facilitate desorption under mild conditions.[12]

Immobilized metal affinity chromatography (IMAC) is primarily based on affinity adsorption and, therefore, possesses advantages and disadvantages associated with this type of separation technology.[13] Notably, the main feature of bioaffinity chromatography is the specificity of the interaction between the protein of interest and the ligand (chelated metal ion, antibody, dye, etc.). With this technology, large amounts of recombinant proteins can be recovered, usually in a single chromatographic step. Contamination by *Eschericia coli* proteins is usually low because such proteins in general lack metal affinity, although some *E. coli* proteins that show metal affinity, such as superoxide dismutase, can interfere with the purification process.[13,14] IMAC has some unique and attractive characteristics:

1. IMAC often allows single-step purification.[13,15]
2. The protein loading capacity is relatively high in comparison with that of other affinity chromatography techniques (0.1–10 m*M*/mL of gel).[13,15,16]
3. The metal ions can be easily removed from the resin with a strong chelating agent such as ethylenediamine tetraacetic acid (EDTA) or ethylene bis (oxyethylene nitrilo) tetraacetic acid (EGTA). Different metal ions can, therefore, be tested, with the same chelating resin, to determine the best ligand for the separation of a protein of interest.
4. IMAC upscaling is fairly easy and reproducible and can be used for industrial applications.[13,15]
5. IMAC is useful for concentrating dilute protein solutions.[13,16]
6. IMAC is compatible with a number of buffers containing high-ionic-force or chaotropic components.[13,16]
7. IMAC in general does not adversely affect the structure of proteins. A few cases have been reported in which metalloenzymes had their essential metal ion stripped off. A case has also been reported in which a protein was damaged by IMAC on a Cu(II)–iminodiacetic acid column, but the damage was triggered by reducing agents that caused oxidative proteolysis catalyzed by Cu(II).[13,16]
8. Upon passage through a noncharged IMAC column, solutions become transiently sterile because all metal ions essential for bacterial growth are removed by chelation.[13,16]
9. An IMAC resin can be regenerated several hundreds of times without a loss of chromatographic characteristics.[13,17] IMAC gels are also extremely sturdy if pH values below 4 are not used.[13]

Magnetic fields have been used in support systems for the study of different applications.[18–20] The use of magnetic particles in bioprocesses has many advantages. They can be easily separated from the reaction medium and stabilized in a fluidized-bed reactor through the application of a magnetic field. The use of magnetic particles reduces capital and operation costs.[19]

In this study, a support matrix with Cu(II)-incorporated magnetic poly(ethylene glycol dimethacrylate-*co*-*N*-Methacryloyl-(L)-histidine methyl ester) [m-p(EGDMA-*co*-MAH)] microbeads was prepared. First, *N*-methacryloyl-(L)-histidine methyl ester (MAH) was synthesized from methacryloyl chloride and histidine. m-p(EGDMA-*co*-MAH) microbeads, 150–250 μm in diameter, were obtained by the suspension polymerization of MAH and ethylene glycol dimethacrylate (EGDMA). Then, Cu(II) ions were incorporated into this carrier for the separation of bovine serum albumin (BSA) from aqueous media. Finally, system parameters, such as the adsorption conditions (i.e., the initial BSA concentration, medium pH, temperature, and ionic strength) were varied to evaluate their effects on the performances of m-p(EGDMA-*co*-MAH)–Cu(II) microbeads.

This novel approach to the preparation of an affinity matrix has many advantages over conventional techniques that require the activation of the matrix for ligand immobilization.[21] In this procedure, MAH acts as the metal-complexing ligand, and there is no need to activate the matrix for ligand immobilization. MAH is polymerized with EGDMA, and no leakage of the ligand is necessary.

EXPERIMENTAL

Materials

BSA (lyophilized, fraction V) was purchased from Sigma (St. Louis, MO). L-Histidine methyl ester and methacryloyl chloride were supplied by Sigma. The monomer EGDMA was obtained from Fluka AG (Buchs, Switzerland), distilled under reduced pressure in the presence of a hydroquinone inhibitor, and stored at 4°C until it was used. Benzoyl peroxide (BPO) was obtained from Fluka. Poly(vinyl alcohol) (PVAL; molecular weight = 100.000, 98% hydrolyzed) was supplied by Aldrich Chemical Co. (Milwaukee,

TABLE I
Recipe and Polymerization Conditions for the Preparation of the m-p(EGDMA-*co*-MAH) Beads with a Swelling Ratio of 40.2% and a Size Range of 150–250 μm

Aqueous dispersion phase	Organic phase	Polymerization conditions
Distilled water: 50 mL PVAL: 0.2 g	MAH: 1000 mg EGDMA: 12.0 mL Fe_2O_3: 0.5 g Toluene: 12.0 mL BPO: 0.1 g	Reactor volume: 100 mL Stirring rate: 600 rpm Temperature and time: first at 65°C for 4 h and then at 90°C for 2 h

WI). All other chemicals were reagent-grade and were purchased from Merck AG (Darmstadt, Germany). All water used in the experiments was purified with a Barnstead (Dubuque, IA) ROpure LP reverse osmosis unit with a high-flow cellulose acetate membrane (Barnstead D2731) followed by a Barnstead D3804 NANOpure organic/colloid removal and ion-exchange packed-bed system. The purified water had a resistance of 18 MΩ/cm.

Methods

Synthesis of MAH

The following experimental procedure was applied for the synthesis of MAH. L-Histidine methyl ester (5.0 g) and 0.2 g of hydroquinone were dissolved in 100 mL of a CH_2Cl_2 solution. This solution was cooled down to 0°C. Triethylamine (12.7 g) was added to the solution. Methacryloyl chloride (5.0 mL) was poured slowly into this solution under a nitrogen atmosphere, and then this solution was stirred magnetically at room temperature for 2 h. At the end of the chemical reaction period, hydroquinone and unreacted methacryloyl chloride were extracted with 10% NaOH. The aqueous phase was evaporated in a rotary evaporator. The residue (i.e., MAH) was crystallized in an ether–cyclohexane mixture and then dissolved in ethyl alcohol.

Preparation of the m-p(EGDMA-*co*-MAH) beads

EGDMA and MAH comonomers were polymerized in a suspension with BPO and PVAL as the initiator and stabilizer, respectively. Toluene was included in the recipe as the diluent (as a pore former) and crosslinker. Table I provides the recipe and polymerization conditions used to obtain copolymer beads in the size range of 150–250 μm. At the end of the polymerization, soluble residues were removed from the polymer by repeated decantation with water and ethyl alcohol. When not in use, the resulting adsorbents were kept under refrigeration in a 0.02% NaN_3 solution to prevent microbial contamination.

Characterization of the magnetic beads

The specific surface area of the beads was determined in a Brunauer-Emmet-Teller apparatus (ASAP 2000 sorptometer, Micrometrics, United States). The average size and size distribution of the beads were determined by screen analysis with Tyler standard sieves.

The water-uptake ratios of the beads were determined in distilled water. The experiment was conducted as follows. Initially dry beads were carefully weighed before being placed in a 50-mL vial containing distilled water. The vial was put into an isothermal water bath with a fixed temperature (25 ± 0.5°C) for 2 h. The beads were taken out of the water, wiped with filter paper, and weighed. The weight ratio of the dry and wet samples was recorded. The water content of the beads was calculated with the following expression:

$$\text{Water-uptake ratio (\%)} = [(W_s \pm W_0)/W_0] \times 100 \quad (1)$$

where W_0 and W_s are the weights of the beads before and after the uptake of water, respectively.

The surface morphology of the polymeric beads was examined with scanning electron microscopy (SEM). Each sample was initially dried in air at 25°C for 7 days before being analyzed. A fragment of the dried bead was mounted on an SEM sample mount and was sputter-coated for 2 min. The sample was then mounted in a Leitz-AMR-1000 scanning electron microscope (Raster Electronen Microscopy, Jena, Germany). The surface of the sample was scanned at the desired magnification to study the morphology of the beads.

To evaluate the degree of MAH incorporation, the synthesized m-p(EGDMA-*co*-MAH) beads were subjected to elemental analysis with a Leco CHNS-932 elemental analyzer (Chicago, IL).

The ^{1}H-NMR spectrum of the MAH monomer was taken in $CDCl_3$ on a JEOL GX-400 300-MHz instrument. The residual nondeuterated solvent ($CHCl_3$) served as an internal reference. The chemical shifts (δ) are reported in parts per million downfield with respect to $CHCl_3$.

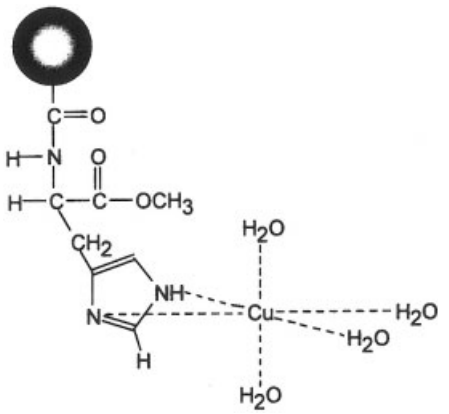

Figure 1 Schematic diagram for the chelation of Cu(II) ions through magnetic beads.

The degree of magnetism of the m-p(EGDMA-*co*-MAH) beads was measured in a magnetic field with a vibrating-sample magnetometer (model 150A, Princeton Applied Research, United States). The presence of magnetite particles in the polymeric structure was investigated with an electron spin resonance (ESR) spectrophotometer (EL 9, Varian, Palo Alto, CA).

Incorporation of Cu(II) ions into m-p(EGDMA-*co*-MAH) microbeads

Chelates of m-p(EGDMA-*co*-MAH) beads with Cu(II) ions were prepared as follows. m-p(EGDMA-*co*-MAH) beads were mixed with aqueous solutions containing 30 ppm Cu(II) ions at a constant pH of 5.0 (adjusted with HCl and NaOH), which was the optimum pH for Cu(II) chelate formation, and at room temperature. A 1000 ppm atomic absorption standard solution (containing 10% HNO_3) was used as the source of Cu(II) ions. The flasks were agitated magnetically at 600 rpm for 1 h (which was sufficient for equilibrium to be attained). The concentration of the Cu(II) ions in the resulting solutions was determined with a graphite furnace atomic absorption spectrophotometer (AA800, PerkinElmer, Bodenseewerk, Germany). The Cu(II) chelation step is depicted in Figure 1. The amount of adsorbed Cu(II) ions was calculated with the concentrations of the Cu(II) ions in the initial solution and in equilibrium.

Cu(II) leakage from the m-p(EGDMA-*co*-MAH) beads was investigated with media of pH 6.0–8.0 and also in a medium containing 1.0*M* NaSCN. The magnetic bead suspensions were stirred for 24 h at room temperature. The Cu(II) concentration was then determined in the supernatants with an atomic absorption spectrophotometer. Immobilized metal-containing beads were stored at 4°C in a 10 m*M* tris (hydroxymethyl)aminomethane HCl buffer (pH 7.4) with 0.02% sodium azide to prevent microbial contamination.

Adsorption studies with BSA

BSA was selected as a model protein. BSA adsorption of the plain and Cu(II)-chelated m-p(EGDMA-*co*-MAH) microbeads were studied at various pH values, either in an acetate buffer (0.1*M*, pH 4.0–5.5) or in a phosphate buffer (0.1*M*, pH 6.0–8.0). The initial BSA concentration was changed between 0.05 and 2.0 mg/mL. In a typical adsorption experiment, BSA was dissolved in 10 mL of the buffer solution containing NaCl, and microbeads were added. The adsorption experiments were carried out for 2 h at 25°C at a stirring rate of 100 rpm. At the end of the equilibrium period (i.e., 2 h), the microbeads were separated from the solution. The BSA adsorption capacity was determined with the Bradford method. The amount of adsorbed BSA was calculated as follows:

$$Q = [(C_0 \pm C)V]/m \quad (2)$$

where Q is the amount of BSA adsorbed per unit of mass of the beads (mg/g); C_0 and C are the concentrations of BSA in the initial solution and in the aqueous phase after the treatment for a certain period of time, respectively (mg/mL); V is the volume of the aqueous phase (mL); and m is the mass of the beads used (g).

Desorption of BSA from Cu(II)-incorporated m-p(EGDMA-*co*-MAH) microbeads

BSA desorption experiments were performed in a buffer solution containing 1.0*M* NaSCN at pH 8.0. The BSA-loaded microbeads were placed in the desorption medium and stirred for 1 h at 25°C at a stirring rate of 100 rpm. The final BSA concentration in the desorption medium was determined by the Bradford method. In the case of Cu(II)-carrying adsorbents, the desorption of Cu(II) ions was also measured in the desorption medium with atomic absorption spectroscopy. The desorption ratio was calculated from the amount of BSA adsorbed onto the microbeads and from the amount of BSA desorbed.

RESULTS AND DISCUSSION

Characterization of the beads

The prepared poly(ethylene glycol dimethacrylate) [p(EGDMA)] and m-p(EGDMA-*co*-MAH) microbeads have a hydrophilic structure. Because EGDMA is compact and forms crosslinks, water diffusion into the polymer matrices is rather difficult. Another reason that water uptake into the structure is limited is the nearness of the polymer chains. Figure 2 shows that the equilibrium swelling is reached in approximately 30 min.

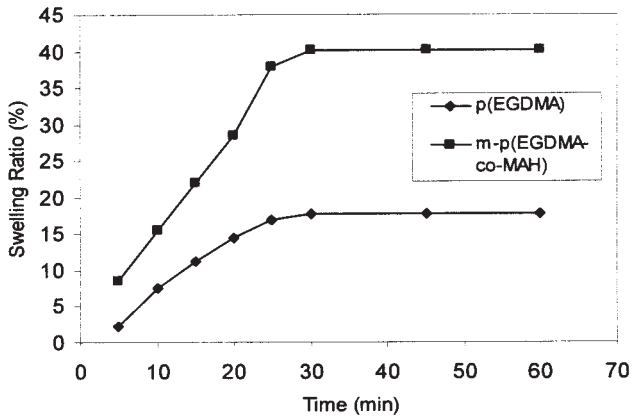

Figure 2 Swelling behavior of p(EGDMA) and m-p(EGDMA-*co*-MAH) microbeads.

When the swelling ratio of the p(EGDMA) microbeads (17.7%) is compared with that of the m-p(EGDMA-*co*-MAH) microbeads, it can be concluded that the swelling rate increases considerably with incorporation into the polymeric structure (40.2%). A few factors may lead to this result. First, the incorporation of MAH into the polymeric structure enables groups that provide more water intake. Second, the reaction of MAH with EGDMA can reduce the molecular weight of the polymer substantially. As a result, water molecules can penetrate the polymer chains more easily, and this leads to more swelling of the polymer in aqueous solutions.

The surface morphology of m-p(EGDMA-*co*-MAH) microbeads is exemplified by the electron micrographs in Figure 3. The polymeric microbeads have a spherical form and rough surface because of the pores that form during the polymerization. Micropores within the microbead surface can be clearly seen in this photograph. The roughness of the microbead surface should be considered a factor providing an increase in the surface area. In addition, these micropores reduce diffusional resistance and facilitate mass transfer because of their high internal surface area. This also provides a higher BSA adsorption capacity. The molecular formula of the newly synthesized m-p(EGDMA-*co*-MAH) microbeads is given in Figure 4.

To evaluate the degree of MAH incorporation into the polymeric structure, an elemental analysis of the synthesized m-p(EGDMA-*co*-MAH) beads was performed. The incorporation of MAH was found to be 43.9 μmol/g polymer with nitrogen stoichiometry. The maximum Cu(II) loading was 4.1 μmol/g polymer.

The radical suspension polymerization procedure provided crosslinked m-p(EGDMA-*co*-MAH) beads in a spherical form, mostly in the size range of 150–250 μm. The specific surface area of the m-p(EGDMA-*co*-MAH) beads was found to be 80.1 m^2/g.

^{1}H-NMR ($CDCl_3$) spectroscopy was used to determine the structure of MAH. The characteristic peaks (δ) were as follows: 1.99 (t, 3H, J = 7.08 Hz, CH_3), 1.42 (m, 2H, CH_2), 3.56 (t, 3H, O—CH_3), 4.82–4.87 (m, 1H, methine), 5.26 (s, 1H, vinyl H), 5.58 (s, 1H, vinyl), 6.86 (1H, J = 7.4 Hz, NH), 7.82 (1H, J = 8.4 Hz, NH), and 6.86–7.52 (m; 5H, aromatic).

The presence of magnetite particles in the polymer structure was confirmed with ESR. The intensity versus the magnetic field (Gauss) is shown in Figure 5.

The application of an external magnetic field, however, may generate an internal magnetic field in the sample that will add to or subtract from the external field. The local magnetic field (H_{local}) generated by the electronic magnetic moment will add vectorially to the external magnetic field (H_{ext}) to produce an effective field (H_{eff}):

$$H_{eff} = H_{ext} + H_{local} \quad (3)$$

Figure 5 shows that the m-p(EGDMA-*co*-MAH) microbeads have a relatively intensity of 120. This value

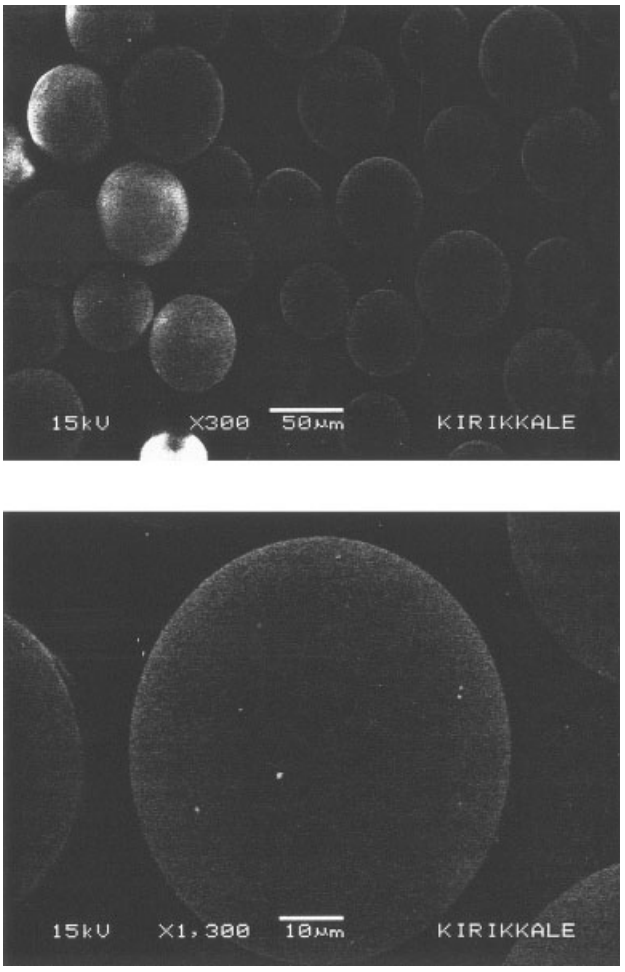

Figure 3 SEM micrographs of m-p(EGDMA-*co*-MAH) microbeads.

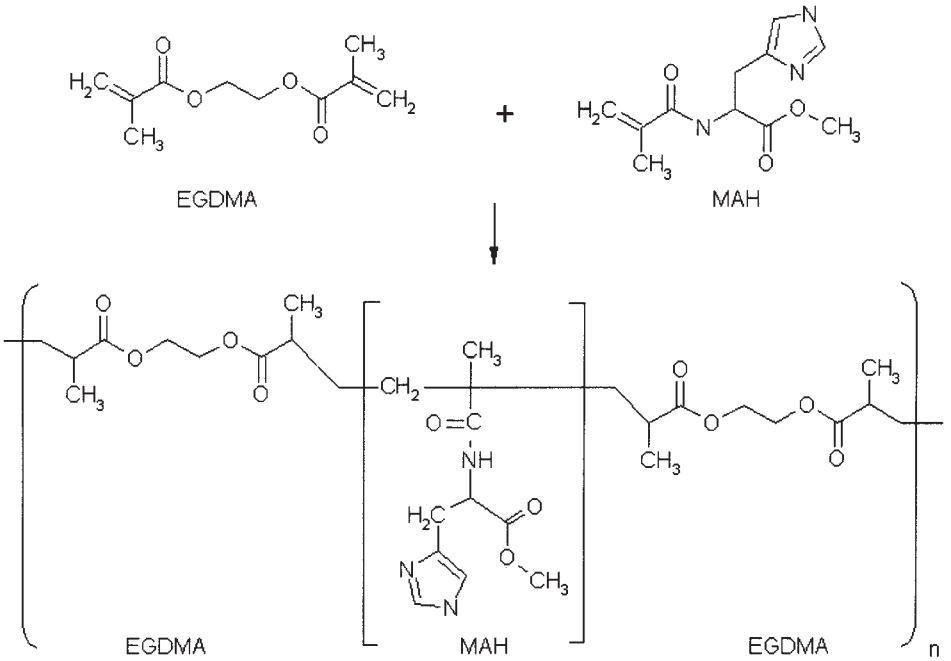

Figure 4 Molecular formula of m-p(EGDMA-*co*-MAH) beads.

shows that the polymeric structure has a local magnetic field because of the magnetite in its structure:

$$g_{\text{eff}} = h\nu/\beta H_r \quad (4)$$

Here, h is the Planck constant (6.626×10^{-27} ergs^{-4}); β is Universal constant (9.274×10^{-21} erg G^{-1}); v is the frequency (9.707×10^{9})H_2); and H_r is resonance of the magnetic field (G).

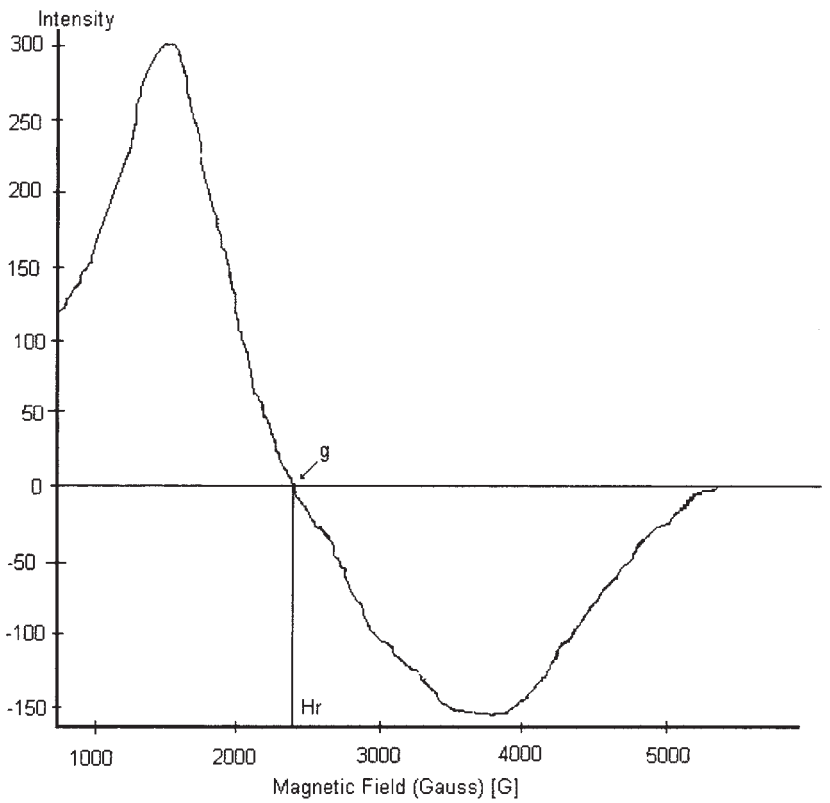

Figure 5 ESR spectrum of m-p(EGDMA-*co*-MAH) microbeads.

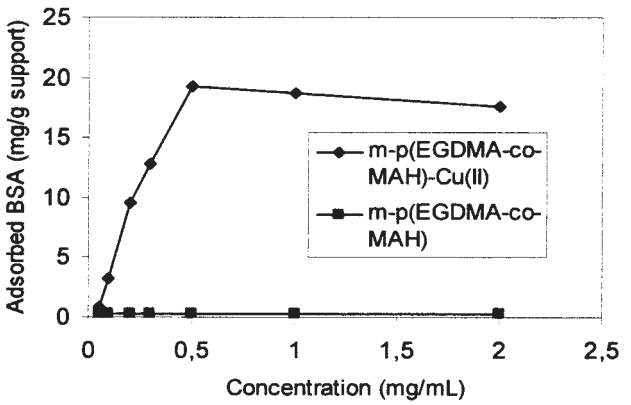

Figure 6 Effects of the initial concentration on the BSA adsorption capacity of metal-chelated m-p(EGDMA-*co*-MAH) [pH = 5.0 for the acetate buffer; MAH concentration = 43.9 μmol/g; Cu(II) loading = 4.1 μmol/g; size = 150–250 μm; incubation time = 2 h].

The *g* factor (Fig. 5) can be considered a quantity characteristic of the molecules in which the unpaired electrons are located, and it is calculated with eq. (4). The measurement of the *g* factor for an unknown signal can be a valuable aid in the identification of the signal origin.[22] In the literature, the *g* factor for Fe^{3+} (low-spin and high-spin complexes) is reported to be 1.4–3.1 and 2.0–9.7, respectively. The *g* factor is 2.56 for the m-p(EGDMA-*co*-MAH) structure.

BSA adsorption/desorption

Adsorption

Figure 6 shows the effects of the initial BSA concentration on the adsorption. The pH of the adsorption medium was 5.0 (i.e., the isoelectric point of BSA), adjusted with the CH_3COONa–CH_3COOH buffer system. The amount of Cu(II) ions loaded on the m-p(EGDMA-*co*-MAH) microbeads was 4.1 μmol/g of polymer. As expected, the BSA adsorption first increased with an increasing initial concentration of BSA in the incubation medium and then reached a saturation value at an initial BSA concentration of 0.5 mg/mL, possibly as a result of the steric hindrance effect. The nonspecific BSA adsorption was very low (0.3 mg of BSA/g of polymer). The Cu(II) incorporation significantly increased the BSA adsorption capacity of the microbeads (up to 19.2 mg of BSA/g of polymer), possibly because of the specific interactions between the BSA molecules and Cu(II) ions.

To determine the effects of the pH on the BSA adsorption, we repeated adsorption experiments at different pH values between 4.0 and 8.0. Figure 7 shows the effects of pHs. The maximum adsorption of BSA was observed around its isoelectric point of pH 5.0. This may be due to a preferential interaction between the BSA molecules and Cu(II) ions at this pH. Significantly lower adsorption capacities were obtained in more acidic and more alkaline pH regions. Proteins have no net charge at their isoelectric points, and so the maximum adsorption from aqueous solutions is usually observed at their isoelectric point.[23]

Figure 8 shows that the nonspecific adsorption of BSA onto m-p(EGDMA-*co*-MAH) was very low at all the temperatures examined. Also, no significant effect of the temperature was observed on the physical adsorption of BSA onto m-p(EGDMA-*co*-MAH). However, the equilibrium adsorption of BSA onto m-p(EGDMA-*co*-MAH)–Cu(II) significantly decreased with increasing temperature. This can be attributed to the chemical interaction between the Cu(II) ions and BSA

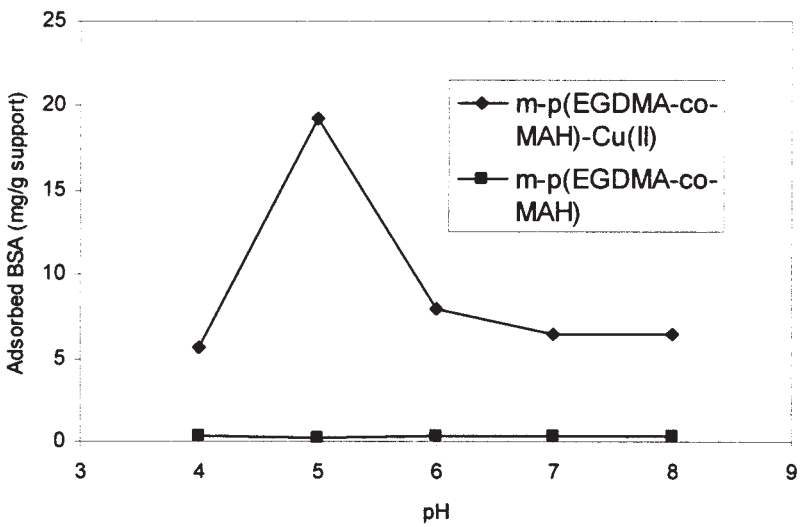

Figure 7 Effects of the pH on the BSA adsorption [BSA concentration = 0.5 mg/mL; MAH concentration = 43.9 μmol/g; Cu(II) loading = 4.1 μmol/g; size = 150–250 μm; incubation time = 2 h].

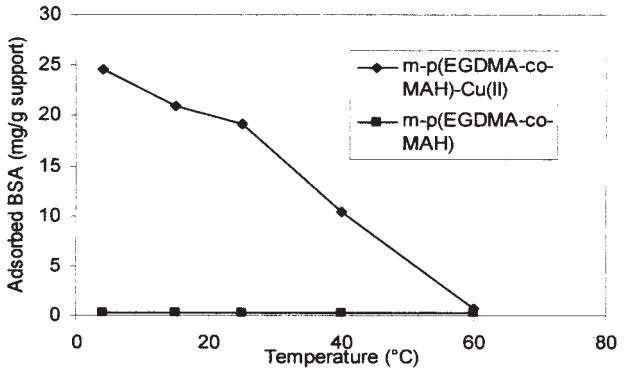

Figure 8 Effect of the temperature on the BSA adsorption [BSA concentration = 0.5 mg/mL; pH = 5.0 for the acetate buffer; MAH concentration = 43.9 μmol/g; Cu(II) loading = 4.1 μmol/g; size = 150–250 μm; incubation time = 2 h].

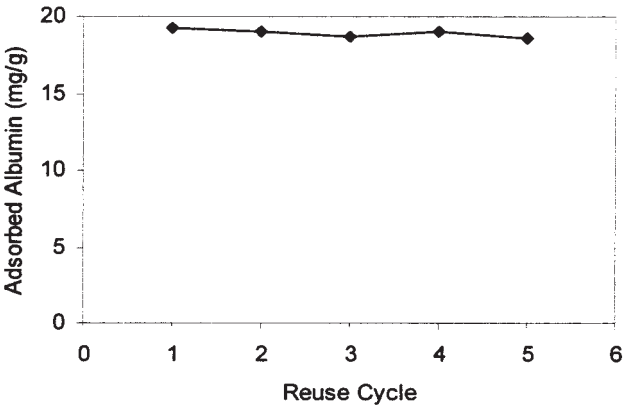

Figure 10 Repeated use of m-p(EGDMA-*co*-MAH)–Cu(II) microbeads [MAH loading = 43.9 μmol/g; Cu(II) loading = 4.1 μmol/g; size = 150–250 μm; initial BSA concentration = 0.5 mg/mL; pH = 5.0; incubation time = 2 h].

as the temperature increased. The thermodynamic factor controlling the specific adsorption process, the overall free energy change associated with binding, probably has a rather complex temperature dependence because this term includes both enthalpy and entropy changes.

The amount of BSA adsorbed onto the beads was reduced as the ionic strength increased in all the cases discussed. Figure 9 shows the effect of the salt concentration on the adsorption capacity of m-p(EGDMA-*co*-MAH)–Cu(II) microbeads. This may be explained by the formation of more compact structures of the BSA molecules at high ionic strengths. More ions may also be attached to BSA molecules at high ionic strengths. This causes further stabilization of the protein molecules (higher solubility), which may lead to lower adsorption of BSA onto the beads.

Desorption

The desorption of adsorbed BSA from m-p(EGDMA-*co*-MAH)–Cu(II) microbeads was studied in a batch experimental setup. The beads, carrying BSA, were placed within a desorption medium containing 1.0*M* NaSCN at pH 8.0, and the amount of BSA and Cu(II) released in 1 h was determined. It was then repeatedly used for the adsorption of BSA. The BSA adsorption capacity did not change during the five successive adsorption–desorption cycles (Fig. 10). The desorption ratios for both BSA and Cu(II) were calculated with the following expression:

$$\text{Desorption ratio (\%)} = \text{Amount of BSA released/Amount of BSA adsorbed on the microsphere} \times 100 \quad (5)$$

These results show that the Cu(II)-incorporated m-p(EGDMA-*co*-MAH)–Cu(II) beads can be repeatedly used in albumin adsorption without detectable losses in their initial adsorption capacities. Note that there was only negligible Cu(II) release in this case, which

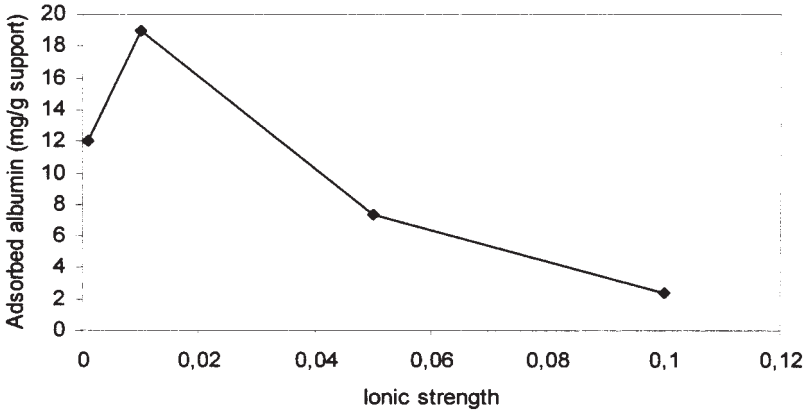

Figure 9 Effect of the salt concentration on the adsorption capacity of m-p(EGDMA-*co*-MAH) microbeads [BSA concentration = 0.5 mg/mL; pH = 5.0 for the acetate buffer; MAH concentration = 43.9 μmol/g; Cu(II) loading = 4.1 μmol/g; size = 150–250 μm; incubation time = 2 h].

shows that the Cu(II) ions were attached to the histidine molecules on the bead surface by strong chelate formation.

CONCLUSIONS

Metal chelate affinity chromatography is a sensitive and selective method for protein separation. The number of locations of surface-exposed electron-donating imidazole and thiol groups and their ability to coordinate with chelated metal ions dictate the adsorption of proteins onto metal-immobilized adsorbents. m-p(EGDMA-*co*-MAH)–Cu(II) beads were used for the adsorption of BSA in a batch system. This novel approach for the preparation of an adsorbent has many advantages over conventional techniques. An expensive and critical step in the preparation process of a metal-chelating adsorbent is the coupling of a chelating ligand to the adsorption matrix. In this procedure, the comonomer MAH acts as the metal-chelating ligand, and there is no need to activate the matrix for chelating-ligand immobilization. Another major issue is the slow release of covalently bonded chelators off the matrix. Metal-chelating-ligand release is a general problem encountered in any adsorption technique, causing a reduction in the adsorption capacity. A metal-chelating-ligand-immobilization step has also been eliminated in this approach. MAH was polymerized with EGDMA, and no leakage of the ligand was necessary. It can be concluded that the Cu(II)-incorporated m-p(EGDMA-*co*-MAH) microbeads may effectively [i.e., with high adsorption capacities for both Cu(II) ions and BSA molecules] be used for the metal chelate affinity separation of BSA. Adsorbed BSA can be desorbed with 1.0*M* NaSCN at pH 8.0.

References

1. Norbert, W. Fundamentals of Clinical Chemistry; Saunders: London, 1976.
2. He, X. M.; Carter, D. C. Nature 1992, 358, 209.
3. Kassab, A.; Yavuz, H.; Odabasi, M.; Denizli, A. J Chromatogr B 2000, 746, 123.
4. Turkova, J. Bioaffinity Chromatography; Elsevier: New York, 1993.
5. Cohn, E. J.; Strong, L. E.; Hughes, W. L.; Mulford, D. J.; Ashworth, J. N.; Melin, M.; Taylor, H. L. J Am Chem Soc 1946, 68, 459.
6. Stotz, J. F.; Rivat, C.; Geschier, C.; Colosett, P.; Streiff, F. Swiss Biotechnol 1990, 8, 7.
7. Şenel, S.; Akgöl, S.; Arica, Y.; Denizli, A. Polym Int 2001, 50, 1143.
8. Kim, M.; Saito, K.; Furusaki, S.; Sugo, T.; Ishigaki, I. J Chromatogr 1991, 586, 27.
9. Baumbach, G. A.; Hammond, D. Biopharm 1992, 5, 24.
10. Huang, P. Y.; Carbonell, R. G. Biotechnol Bioeng 1999, 63, 633.
11. Huang, P. Y.; Carbonell, R. G. Biotechnol Bioeng 1995, 47, 288.
12. Huang, P. Y.; Baumbach, G. A.; Dadd, C. A.; Buettner, J. A.; Hentsch, M.; Masecar, B. L.; Hammond, D. J.; Carbonell, R. G. Bioorg Med Chem 1996, 4, 699.
13. Ueda, E. K. M.; Gout, P. W.; Morganti, L. J Chromatogr A 2003, 988, 1.
14. Sawadogo, M.; Van Dyke, M. W. Genet Eng 1995, 17, 53.
15. Arnold, F. H. Biotechnol 1991, 9, 151.
16. Bush, K. D.; Lumpkin, J. A. Biotechnol Prog 1998, 14, 943.
17. Porath, J. Trends Anal Chem 1988, 7, 254.
18. Bahar, T.; Celebi, S. S. Enzyme Microb Technol 2000, 26, 28.
19. Akgöl, S.; Kacar, Y.; Denizli, A.; Arıca, M. Y. Food Chem 2001, 74, 281.
20. Akgöl, S.; Yalçınkaya, Y.; Bayramoğlu, G.; Denizli, A.; Arica, Y. Process Biochem 2002, 38, 675.
21. Denizli, A.; Salih, B.; Pişkin, E. J Appl Polym Sci 1997, 65, 2085.
22. Swartz, H. M.; Bolton, J. R.; Borg, D. C. Biological Applications of Electron Spin Resonance; Wiley: New York, 1972.
23. Shirahama, H.; Shikawa, T.; Suzawa, T. Colloid Polym Sci 1989, 267, 587.